Ultrasound-Based Prediction Model for Distinguishing Malignant from Benign Thyroid Nodules with Peripheral Calcification

Song Bai, MD[1] Linghu Wu, MD[1] Youhuan Su, MD, Jinfeng Xu, MD, Fajin Dong, MD

Rationale and Objectives: The differential diagnosis of thyroid nodules with peripheral calcifications by ultrasound (US) has always been source of confusion. This study aimed to develop and validate a predictive US-based nomogram model to differentiate malignant from benign nodules with peripheral calcifications.

Methods: Of the 8359 thyroid nodules scanned by ultrasonography between January 2017 and January 2025, 380 nodules with peripheral calcifications were included, with confirmed pathological results and US examinations. 268 nodules were included in the training cohort, and 112 nodules were included in the validation cohort. The candidate variables included age, gender, and the image features obtained from grayscale US. Independent risk factors for malignant thyroid nodules were determined by univariate and multivariate analyses, and a predictive nomogram model was developed. The performance of the US nomogram was assessed by the area under the curve (AUC), calibration curve, and decision curve analysis (DCA) results.

Results: Univariate and multivariate logistic regression analyses revealed that the halo sign, extrusion beyond calcification, type of peripheral calcification, margin, internal echogenicity, and composition were significant independent predictors for malignant thyroid nodules with peripheral calcifications. The nomogram model based on the six variables exhibited excellent calibration and discrimination in the training and validation cohorts, with AUC values of 0.904 and 0.882, respectively. The DCA showed that a probability threshold of 0.11–0.83 could benefit patients clinically.

Conclusion: The US-based nomogram model can potentially predict the malignant risk of thyroid nodules with peripheral calcifications, thereby helping to enhance diagnostic accuracy.

Key Words: Thyroid nodules; Ultrasonography; Peripheral calcifications; Nomogram.

INTRODUCTION

The incidence of thyroid nodules (TNs) is increasing substantially worldwide in recent decades, primarily attributed to advances in diagnostic imaging. Driven by the widespread adoption of ultrasound (US) screening, their detection rates have increased rapidly, with epidemiological data indicating a prevalence ranging from 19% to 68% (1). Thyroid nodules have various types of calcifications, including peripheral calcification, microcalcification, and coarse calcification. Peripheral calcification, a special form of thyroid nodule calcification, is usually pathologically based on dystrophic calcification, which has been considered a characteristic of benign thyroid lesions (2). In recent years, with the deepening of research, this view has been gradually overturned. Peripheral ring or arc calcification has been reported in cases of papillary, undifferentiated, or follicular carcinomas (3–5). Although the correlation between thyroid malignancy and peripheral calcification has been well established, there is no unified statement about the associations of related features of peripheral calcification with malignancy. Features such as the continuity of peripheral calcification are associated with an increased risk of thyroid

Acad Radiol 2025; 32:4486–4499

From the Department of Ultrasound, Shenzhen People's Hospital, Shenzhen 518020, Guangdong, China (S.B., L.W., Y.S., J.X., F.D.); Department of Ultrasound, The Second Clinical Medical College, Jinan University (Shenzhen People's Hospital), Shenzhen 518020, Guangdong, China (J.X., F.D.); Department of Ultrasound, Shenzhen People's Hospital, Longhua Branch, Shenzhen 518020, Guangdong, China (F.D.). Received April 2, 2025; revised April 25, 2025; accepted April 29, 2025. **Address correspondence to:** F.D. e-mail: dongfajin@szhospital.com

[1] These authors contributed equally to this work.

https://doi.org/10.1016/j.acra.2025.04.073

malignancy (6,7). Kwak et al. and Yoon et al. divided peripheral calcification into three types and reported no significant differences among the three types of peripheral calcification (8,9). Malhi et al. also reported that specific peripheral marginal calcification features did not help distinguish benign nodules from malignant nodules (10). These conflicting results may be due to the insufficient sample size and incomplete analysis of ultrasound (US) features, which can confuse clinicians in their diagnosis. To the best of our knowledge, no previous studies have examined whether US nomograms can more effectively distinguish benign and malignant TNs with peripheral calcifications.

In this study, we evaluated a relatively large number of cases of TNs and integrated US features with clinical characteristics to investigate predictive factors associated with malignant TNs with peripheral calcifications. These factors were used to develop and validate an easy-to-use nomogram model to improve diagnostic accuracy.

MATERIALS AND METHODS

Patients

This retrospective study was approved by our institutional review board. Patient approval or informed consent is not required to review medical records or images. All patients signed an informed consent form before US-guided fine-needle aspiration (FNA) and surgery.

From January 2017 to January 2025, a total of 8359 thyroid nodules diagnosed with calcification from consecutive patients were reviewed. All the data were extracted from the electronic medical records system and ultrasound report database and did not show any personally identifiable information. The search keywords in the ultrasound report database were set as "hyperechoic"/ "calcification" and "thyroid" to include as many potentially eligible cases as possible. The pathology of all thyroid nodules included in this study was confirmed by cytologic results from FNA, histopathological results from surgery, or both. One radiologist (S.B), who was blinded to the final pathologic results and the ratio of malignant to benign nodules, retrospectively reviewed the sonographic data of the 373 patients and identified thyroid nodules with peripheral calcifications.

The inclusion criteria were as follows: (1) complete clinical and thyroid ultrasound imaging data; (2) the nodule was analyzed according to surgical histology within 1 month after examination; and (3) confirmed cytological (e.g., Bethesda category II and VI nodules) or histopathological results were available. The exclusion criteria were as follows: (1) inadequate cytologic results (e.g., Bethesda category I nodules) and no surgical histology; (2) indeterminate cytologic results (for Bethesda category III, IV, or V) and no surgical histology; (3) history of therapy (radiofrequency ablation or neck radiation therapy); and (4) nodules with unclear ultrasound images. Because microcalcifications are more likely to be malignant, when microcalcifications occur in a lesion along with peripheral calcifications, the lesion was excluded from the study. Finally, a total of 380 nodules from 373 patients (86 men and 287 women) were included in our study. Figure1 shows the flowchart of the patient enrollment process.

US Examinations

All US examinations were conducted using the EPIQ5/7/Elite systems (Philips Medical Systems, Bothell, WA) with a 5–12 MHz linear transducer, LOGIQ E9/S8 systems (General Electric Healthcare, Milwaukee, WI) with a 6–15 MHz linear transducer, Resona 7 series systems (Mindray Biomedical Electronics, Shenzhen, China) with a 3–9/3–11/5–14 MHz linear transducer, Resona R9 series systems (Mindray Biomedical Electronics, Shenzhen, China) with a 3–15 MHz linear transducer, DC series systems (Mindray Biomedical Electronics, Shenzhen, China) with a 3–12 MHz linear transducer, ACUSON S2000 system (Siemens, Erlangen, Germany) with a 5–14 MHz linear transducer, Aixplorer system (SonoScape Medical Corp., Shenzhen, China) with a 4–15/2–10 MHz linear transducer, and S60 Maso system (SonoScape Medical Corp., Shenzhen, China) with a 3–12 MHz linear transducer. Patients were examined in the supine position with their necks exposed. Grayscale US was performed to evaluate the position, size, and ultrasonic characteristics of the nodules. Cross-sectional and longitudinal images of the target nodules were recorded. All the sonograms were classified by two doctors (S.B. and L.H.W.) who have more than 10 years of working experience without knowing the pathological results, and any disagreements were resolved through discussion with a senior doctor (F.J.D.). US images were randomly provided to the reviewers on the US system workstation.

Image Analysis

The selection of ultrasound features in our analysis was primarily based on the American College of Radiology thyroid imaging reporting and data system (ACR TI-RADS) criteria, with vascularity not included. The following US features were analyzed for each nodule: size (maximum diameter, ≤1 cm, >1 cm to ≤2 cm, or >2 cm), shape (longitudinal diameter/transverse diameter [L/T] ratio, ≤1 or >1), internal echogenicity (hypoechoic, isoechoic/hyperechoic compared to the background thyroid gland or invisible because of posterior acoustic attenuation), internal calcification (none or large comet-tail, macrocalcification, or invisible), composition (solid-cystic, solid or invisible), margin (regular, irregular/lobulated or invisible), halo sign (present or absent), range of peripheral calcification (circular or arc), extrusion beyond calcifications (yes or no), calcification continuity (interrupted or continuous) and type of peripheral calcification.

According to the surface characteristics, peripheral calcifications were classified into one of the following three categories: type I, coarse calcification (curvilinear, smooth surface, even thickness); type II, coarse calcification (curvilinear, rough surface, uneven thickness); and type III,

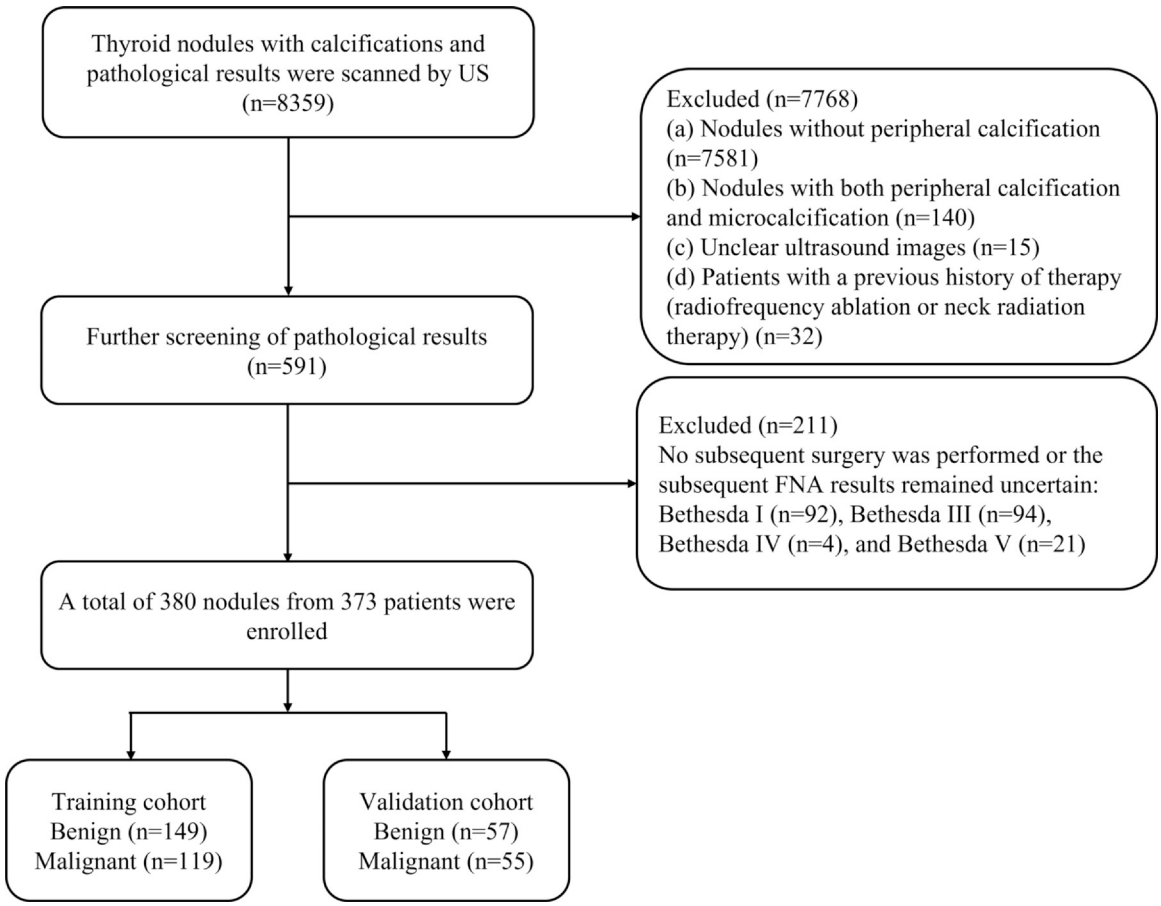

Figure 1. Flowchart of the patient enrollment process. FNA, fine-needle aspiration; US, ultrasound.

stippled (small and non-linear calcification spots). The boundary between coarse and small calcifications was 2 mm in diameter. The nodules were also classified as arc or circular based on the range of the calcifications around the nodule border. Circular refers to the sum of calcification length ≥2/3 of the nodule margin; arc refers to the sum of calcification length < 2/3 of the nodule margin.

Statistical Analysis

For statistical descriptions, categorical variables are presented as n (%), and continuous variables are presented as the means with standard errors or medians with quantile values (Q1, Q3). For continuous variables, Student's t test was used if the variable was normally distributed; otherwise, the Mann−Whitney U test was used. χ^2-tests or Fisher's exact test were used to compare the categorical variables.

Multivariate logistic regression was performed on variables that were statistically significant in the univariate analysis. A predictive model was developed based on multivariate logistic regression and presented as a nomogram. Odds ratios (ORs) with 95% confidence intervals (CIs) and P-values were calculated. The ability of the model to discriminate was assessed according to the area under the curve (AUC) and goodness-of-fit of the nomogram via the Hosmer–Lemeshow test. The C-index and a calibration curve were generated to assess the agreement of the nomogram-predicted probability with the actual observed probability. Decision curve analysis (DCA) was performed to obtain the final ranges for threshold probabilities to compare the efficacies of the nomograms. In cases of nodules with posterior acoustic shadowing, multiple imputation was applied to the missing data, and the table reflects the post-imputation dataset. Before the validation dataset was evaluated, the training dataset was internally validated through bootstrap resampling. All the statistical significance tests were two-tailed and statistical significance was set as $P < 0.05$.

Cohen's k was used to test the agreement between radiologists for the evaluation of nodules. The k coefficients were evaluated using the following method (11): 0≤k≤0.4: poor; 0.41≤k≤0.75: fair to good; 0.76≤k < 1.0: excellent; and k=1.0: perfect. Analyses were performed using SPSS Version 23 (IBM, Armonk, NY, USA) and R software (Ri386 4.0.3, R Foundation for Statistical Computing, Vienna, Austria).

RESULTS

Clinicopathological Data and US Characteristics

The detailed clinicopathological data and US characteristics of patients in the training and validation datasets are listed in

Table 1. A total of 206 benign nodules in 202 patients and 174 malignant nodules in 172 patients were randomly divided in a 7:3 ratio into training and validation datasets (n = 268 and n = 112, respectively). The median (Q1, Q3) patient age was 47.00 (37.00,57.00) years for the training cohort, and 47.00 (36.00, 54.25) years for validation

TABLE 1. Baseline Conventional Ultrasound and Clinical Data of Patients in the Training and Validation Cohorts

Variables	Training Cohort (n = 268)			Validation Cohort (n = 112)		
	Benign (n = 149)	Malignant (n = 119)	P-value	Benign (n = 57)	Malignant (n = 55)	P-value
Gender, n (%)						
Female	129 (86.6)	85 (71.4)		44 (77.2)	33 (60.0)	
Male	20 (13.4)	34 (28.6)	0.002	13 (22.8)	22 (40.0)	0.050
Age(years), median (Q1, Q3)	51.0 (41.0, 59.0)	45.0 (34.0, 53.0)	0.002	50.0 (41.0,58.0)	44.0 (35.0, 51.0)	0.019
Maximum diameter(cm), n (%)						
≤1cm	80 (53.7)	65 (54.6)		27 (47.4)	31 (56.4)	
>1 cm to ≤2cm	46 (30.9)	46 (38.7)		21(36.8)	21 (38.2)	
>2 cm	23 (15.4)	8 (6.7)	0.063	9 (15.8)	3 (5.5)	0.198
Range of peripheral calcification, n (%)						
Arc	86 (57.7)	63 (52.9)		33 (57.9)	35 (63.6)	
Circular	63 (42.3)	56 (47.1)	0.434	24 (42.1)	20 (36.4)	0.534
Halo sign, n (%)						
Absent	99 (66.4)	58 (48.7)		40 (70.2)	26 (47.3)	
Present	50 (33.6)	61 (51.3)	0.003	17 (29.8)	29 (52.7)	0.014
Extrusion beyond calcification, n (%)						
No	142 (95.3)	87 (73.1)		54 (94.7)	44 (80.0)	
Yes	7 (4.7)	32 (26.9)	<0.001	3 (5.3)	11 (20.0)	0.018
Calcification continuity, n (%)						
Continuous	52 (34.9)	21 (17.6)		21 (36.8)	13 (23.6)	
Interrupted	97 (65.1)	98 (82.4)	0.002	36 (63.2)	42 (76.4)	0.129
Type of peripheral calcification, n (%)						
Type 1 coarse calcification (curvilinear, smooth surface, even thickness)	88 (59.1)	10 (8.4)		36 (63.2)	6 (10.9)	
Type 2 coarse calcification (curvilinear, rough surface, uneven thickness)	54 (36.2)	59 (49.6)		17 (29.8)	28 (50.9)	
Type 3 stippled	7 (4.7)	50 (42.0)	<0.001	4 (7.0)	21 (38.2)	<0.001
L/T ratio, n (%)						
≤1	143 (96.0)	102 (85.7)		56 (98.2)	49 (89.1)	
>1	6 (4.0)	17 (14.3)	0.003	1 (1.8)	6 (10.9)	0.045
Margin, n (%)						
Regular	125 (83.9)	38 (31.9)		52(91.2)	26 (47.3)	
Irregular/lobulated	24 (16.1)	81 (68.1)	<0.001	5 (8.8)	29 (52.7)	<0.001
Internal echogenicity, n (%)						
Isoechoic/Hyperechoic	76 (51.0)	10 (8.4)		31 (54.4)	5 (9.1)	
Hypoechoic	73 (49.0)	109 (91.6)	<0.001	26 (45.6)	50 (90.9)	<0.001
Composition, n (%)						
Solid-cystic	52 (34.9)	5 (4.2)		14 (24.6)	5 (9.1)	
Solid	97 (65.1)	114 (95.8)	<0.001	43 (75.4)	50 (90.9)	0.029
Internal calcification, n (%)						
None or large comet-tail	131 (87.9)	104 (87.4)		53 (93.0)	44 (80.0)	
Macrocalcification	18 (12.1)	15 (12.6)	0.897	4 (7.0)	11 (20.0)	0.044

L/T, longitudinal diameter/transverse diameter

cohort. Both the training and validation datasets exhibited similar malignancy rates (44.4% and 49.1%, respectively; P = 0.40), indicating balanced cohort characteristics.

Among the 206 benign nodules, 122 were cytologically confirmed, 66 were histopathologically confirmed, and 18 were confirmed using both methods. Among the 174 malignant nodules, 10 were cytologically confirmed, 59 were histopathologically confirmed, and 105 were confirmed by both methods. All 174 malignant nodules were diagnosed as papillary carcinoma. Of the 206 benign nodules, 65 were diagnosed as nodular goiter, 12 as follicular adenoma, 1 as Hashimoto's thyroiditis, 5 as fibrotic calcification, 1 as atypical hyperplasia, and 122 as cytologically benign. Additionally, one patient was found to have both a benign nodule and a malignant nodule. Among all nodules, 71 nodules exhibited posterior acoustic shadowing, of which 24(33.8%) were malignant and 47(66.2%) were benign.

Establishment of the Nomogram Prediction Model

The results of the univariate and multivariate logistic regression analysis of the training cohort are shown in Table 2. Due to the influence of calcified rings and acoustic shadows, the internal echoes, internal components, internal calcifications, and margins of the 71 nodules in this study could not be evaluated, and we performed multiple imputations for missing values on these nodules. Univariate logistic regression was conducted with 13 variables in the training set. Overall, 11 predictive variables were significantly associated with thyroid malignancy. After multivariate analysis, six variables (halo sign, extrusion beyond calcification, type of peripheral calcification, margin, internal echogenicity, and composition) were found to be significant independent predictors for thyroid malignancy ($p < 0.05$). The Hosmer–Lemeshow test showed that the P value was 0.276, indicating that the model had an increased goodness of fit. On the basis of these independent factors, a nomogram for predicting the malignant risk of TNs with peripheral calcifications was generated (Fig 2). According to the nomogram, type III peripheral calcification was the best predictor of thyroid malignancy, with an odds ratio (OR) of 36.70. The halo sign had the least impact on the nomogram, with an OR of 2.23. Each feature among the variables was assigned a score according to the point scale. The risk probability for malignancy for each patient was calculated by adding the total score and locating it on the total point scale.

Performance of the Nomogram Model

The predictive properties were tested in both the training and validation datasets. The nomogram showed excellent predictive properties, with an AUC of 0.904, a sensitivity of 0.933, a specificity of 0.698, a PPV of 0.712, and an NPV of 0.929 for the training set (Fig 3). For the validation set, the developed nomogram still showed good discrimination with an AUC of 0.882, a sensitivity of 0.909, a specificity of 0.737, a PPV of 0.769, and an NPV of 0.894 (Fig 3).

The calibration curve showed good agreement between the predicted and observed probabilities of malignancy in the training and validation cohorts (Fig 4a–b). The C-index values in the training and the validation cohort were 0.904 (95%CI:0.869–0.938) and 0.882 (95%CI:0.818–0.946,) respectively, which demonstrated satisfactory accuracy for estimating the risk of malignancy.

Clinical Usefulness

The DCA demonstrated that the nomogram exhibited an optimal net benefit in predicting malignancy for threshold probabilities within the range of 11%–83% (Fig 5).

Agreement Among Radiologists

Cohen's kappa coefficient indicated a high degree of agreement among the radiologists (range, 0.76–0.89) (Table 3).

Examples of the Nomogram in Use

For example, the risk of malignancy in Patient 1, who had a nodule with type I calcification, regular margin, isoechogenicity, solid composition, and without halo sign and extrusion beyond calcification (Fig 6a), had a malignant risk of 4% (Fig 6b). Pathology proved that it was benign.

Patient 2, who had a nodule with type I calcification, regular margin, isoechogenicity, solid-cystic composition, and without halo sign and extrusion beyond calcification (Fig 6c), had a malignant risk of < 1% (Fig 6d). Pathology confirmed that it was a nodular goiter with adenomatous hyperplasia.

Patient 3, who had a nodule with type II calcification, halo sign, regular margin, hypoechogenicity, solid composition, and without extrusion beyond calcification (Fig 6e), had a malignant risk of 55% (Fig 6f). Pathology confirmed that it was a papillary thyroid carcinoma.

Patient 4, who had a nodule with type II calcification, halo sign, extrusion beyond calcification, irregular margin, hypoechogenicity, and solid composition (Fig 6g), had a malignant risk of 90% (Fig 6h). Pathology confirmed that it was a papillary thyroid carcinoma.

Patient 5, who had a nodule with type III calcification, irregular margin, hypoechogenicity, solid composition, and without halo sign and extrusion beyond calcification (Fig 6i), had a malignant risk of 91% (Fig 6j). Pathology confirmed that it was a papillary thyroid carcinoma.

DISCUSSION

The association between malignant thyroid lesions and peripheral calcification has been well established. Yoon et al. (8) found that among 65 thyroid lesions with peripheral calcification, 12 (18%) were malignant. Taki et al. (12) reported that 43% of thyroid nodules with peripheral calcification were pathologically confirmed as malignant. In our study,

TABLE 2. Results of the Univariate and Multivariate Analysis Based on the Training Cohort

Variables	Univariate Analysis				Multivariate Analysis	
	Benign (*n* = 149)	Malignant (*n* = 119)	OR (95%CI)	P-value	OR (95%CI)	P-value
Gender, n (%)						
Female	129 (86.6)	85 (71.4)	Reference		Reference	
Male	20 (13.4)	34 (28.6)	2.58 (1.39–4.78)	0.003	1.78 (0.76–4.18)	0.186
Age(years), median (Q1, Q3)	51.0 (41.0, 59.0)	45.0 (34.0, 53.0)	0.97 (0.95–0.99)	0.003	1.00 (0.97–1.03)	0.889
Maximum diameter(cm), n (%)						
≤1cm	80 (53.7)	65 (54.6)	Reference			
>1 cm to ≤2cm	46 (30.9)	46 (38.7)	1.23 (0.73–2.08)	0.437		
>2 cm	23 (15.4)	8 (6.7)	0.43 (0.18–1.02)	0.056		
Range of peripheral calcification, n (%)						
Arc	86 (57.7)	63 (52.9)	Reference			
Circular	63 (42.3)	56 (47.1)	1.21 (0.75–1.97)	0.434		
Halo sign, n (%)						
Absent	99 (66.4)	58 (48.7)	Reference		Reference	
Present	50 (33.6)	61 (51.3)	2.08 (1.27–3.42)	0.004	2.23(1.06–4.70)	0.035
Extrusion beyond calcification, n (%)						
No	142 (95.3)	87 (73.1)	Reference		Reference	
Yes	7 (4.7)	32 (26.9)	7.46 (3.16–17.64)	<0.001	4.36 (1.43–13.32)	0.010
Calcification continuity, n (%)						
Continuous	52 (34.9)	21 (17.6)	Reference		Reference	
Interrupted	97 (65.1)	98 (82.4)	2.50 (1.40–4.47)	0.002	0.54 (0.22–1.28)	0.159
Type of peripheral calcification, n (%)						
Type 1 coarse calcification (curvilinear, smooth surface, even thickness)	88 (59.1)	10 (8.4)	Reference		Reference	
Type 2 coarse calcification (curvilinear, rough surface, uneven thickness)	54 (36.2)	59 (49.6)	9.62 (4.54–20.38)	<0.001	4.39 (1.69–11.37)	0.002
Type 3 stippled	7 (4.7)	50 (42.0)	62.86 (22.52–175.43)	<0.001	36.70 (9.96–135.29)	<0.001
L/T ratio, n (%)						
≤1	143 (96.0)	102 (85.7)	Reference		Reference	
>1	6 (4.0)	17 (14.3)	3.97 (1.51–10.42)	0.005	1.78 (0.50–6.42)	0.377
Margin, n (%)						
Regular	125 (83.9)	38 (31.9)	Reference		Reference	
Irregular/lobulated	24 (16.1)	81 (68.1)	11.10 (6.20–19.88)	<0.001	2.39 (1.08–5.30)	0.032
Internal echogenicity, n (%)						
Isoechoic/Hyperechoic	76 (51.0)	10 (8.4)	Reference		Reference	
Hypoechoic	73 (49.0)	109 (91.6)	11.35 (5.51–23.38)	<0.001	3.05 (1.10–8.43)	0.032

Table 2 (*Continued*)

Variables	Univariate Analysis				Multivariate Analysis	
	Benign (*n* = 149)	Malignant (*n* = 119)	OR (95%CI)	P-value	OR (95%CI)	P-value
Composition, n (%)						
Solid-cystic	52 (34.9)	5 (4.2)	Reference		Reference	
Solid	97 (65.1)	114 (95.8)	12.22 (4.70–31.81)	< 0.001	6.18 (1.50–25.40)	0.012
Internal calcification, n (%)						
None or large comet-tail	131 (87.9)	104 (87.4)	Reference			
Macrocalcification	18 (12.1)	15 (12.6)	1.05 (0.51–2.18)	0.897		

CI, confidence interval; L/T, longitudinal diameter/transverse diameter; OR, odds ratio.

the incidence of malignant thyroid nodules with peripheral calcification was 45.8%, which was higher than that in the previous reports, and this may be because most nodules likely to be benign were classified as TI-RADS category 3 and remained stable during clinical observation, thus not undergoing further puncture or surgery. Consequently, the proportion of malignancy may have been overestimated. Nevertheless, it also reminds researchers that the diagnosis of malignant nodules should not be ruled out on the basis of peripheral calcification alone.

In this study, we developed an ultrasound model for differentiating malignant from benign thyroid nodules with peripheral calcifications. The nomogram showed favorable discriminative value in both the training and validation cohorts. Additionally, the model exhibited good agreement in calibration and had the best net benefit within a reasonable range of threshold probabilities. These results showed that our nomogram can greatly increase the accuracy and efficacy of predicting malignant nodules with peripheral calcifications for clinicians.

In our study, similar to other thyroid nodules, the internal echogenicity, internal composition, and margin contributed to the diagnosis of malignant thyroid nodules with peripheral calcifications. Consistent with previous studies, solid structures were significantly associated with a higher risk of malignancy in peripheral calcified nodules (13,14). Researchers usually consider cystic lesions benign unless a solid component is present. The pathological explanation for this finding may be that benign calcification may occur because of the proliferation of fibrous tissue in the thyroid gland that occurs in benign thyroid disease during the alternating process of hyperplasia and regression. This process affects blood flow to thyroid follicles, resulting in thyroid hemorrhage, necrosis, and cystic degeneration of the nodule after hematoma resorption, resulting in calcification of the nodule wall or calcification of the fibrous septal bands, which leads to the appearance of large coarse calcifications or peripheral calcifications on ultrasound (15,16). In conclusion, the presence of both cystic components and solid structures in thyroid nodules with peripheral calcification may reduce the risk of malignancy compared to the solid component alone. Internal echogenicity is one of the most important indicators for assessing the risk of malignancy of a nodule in thyroid ultrasonography. Hypoechoic and extremely hypoechoic echoes are strongly associated with an increased risk of thyroid malignancy, whereas isoechoic and hypoechoic nodules are associated with a lower risk of malignancy. It is widely recognized that irregular margin is also a significant predictor of thyroid malignancy (17–19), which is consistent with our finding. These findings are also consistent with the ACR TI-RADS guidelines, which state that scores of peripheral calcifications in combination with these characteristics are higher than those of peripheral calcification alone (16).

In our study, no relationship between gender or age and the risk of malignancy was observed in thyroid nodules with peripheral calcifications. The incidence of thyroid cancer is

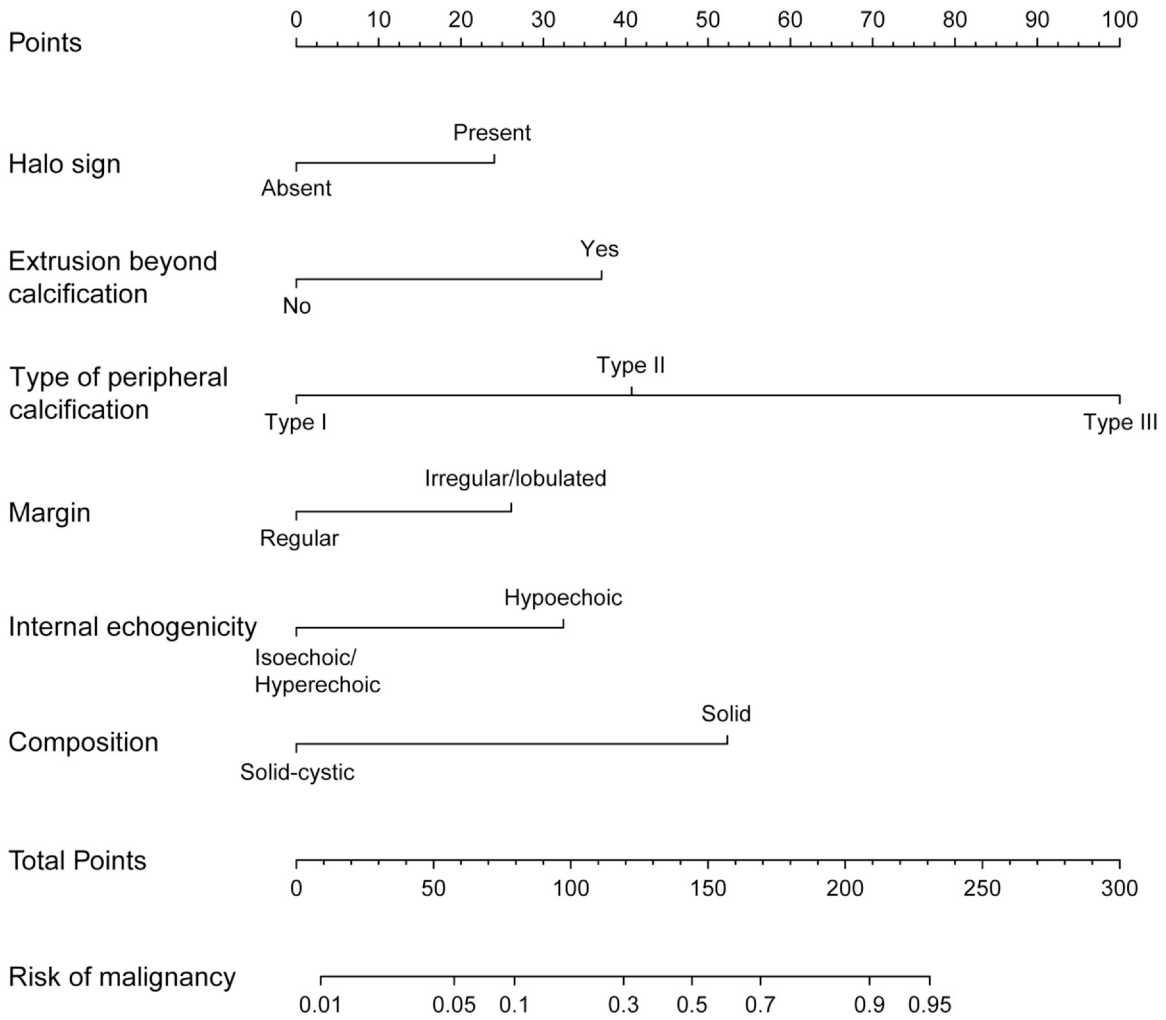

Figure 2. Nomogram for estimating the risk of malignancy of thyroid nodules with peripheral calcifications. Type I, coarse calcification (curvilinear, smooth surface, even thickness); type II, coarse calcification (curvilinear, rough surface, uneven thickness); and type III, stippled (small and non-linear calcification spots).

significantly higher in females than in males, and is particularly common in young women (20–23). The reason for this discrepancy may be that these data focused on all thyroid nodules, whereas our study focused specifically on thyroid nodules with peripheral calcifications. According to our findings, the size of thyroid nodules is also not an independent predictor of malignancy in peripheral calcified nodules. Conflicting findings exist regarding the effect of size on thyroid cancer risk. Some literature suggested that the risk of malignancy in thyroid nodules did not significantly correlate with their size, but depended more on other ultrasound features (14,16,24). It has also been found that the larger the thyroid nodule is, the higher the risk of malignancy. The risk of malignancy for nodules > 1 cm in diameter is much higher than that for nodules < 1 cm in diameter (16). In the contrast, some scholars suggested that subcentimeter nodules with peripheral calcifications also had a high incidence of malignancy (25). Some of these small nodules may not fulfill TI-RADS criteria for biopsy or follow up so distinguishing these peripherally calcified nodules into higher-risk lesions would be helpful.

Because microcalcifications greatly increase the risk of malignancy in thyroid nodules, we compared only coarse calcifications and no calcifications. Coarse calcification was usually considered a diagnostic indicator of benign thyroid lesions in previous studies, but in recent years, coarse calcification has been reported in both benign and malignant nodules (14–16). Kim et al. reported that 66% (116/174) of coarsely calcified nodules were malignant (26). However, in our study, coarse calcification did not increase the risk of malignant nodules, probably because of the low proportion of malignant nodules with coarse calcification in the selected sample. On the other hand, the accuracy of coarse calcification in the diagnosis of malignant nodules is relatively low and is of little significance in the diagnosis of benign and malignant nodules, which need to be differentiated by other sonographic features. The risk of malignancy is significantly increased in nodules with an L/T ratio > 1, with a sensitivity

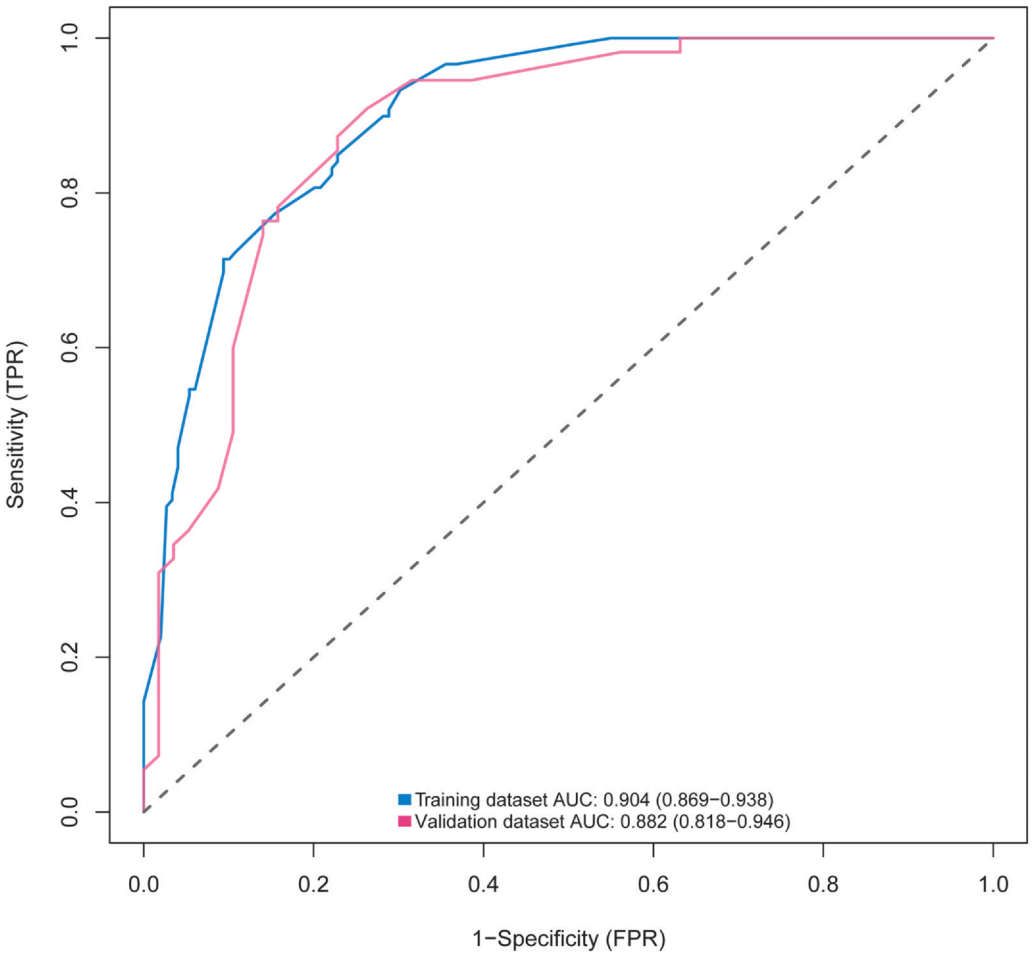

Figure 3. Receiver operating characteristic curves based on the nomogram for malignant thyroid nodules with peripheral calcifications in the training and validation cohorts. AUC, area under the curve.

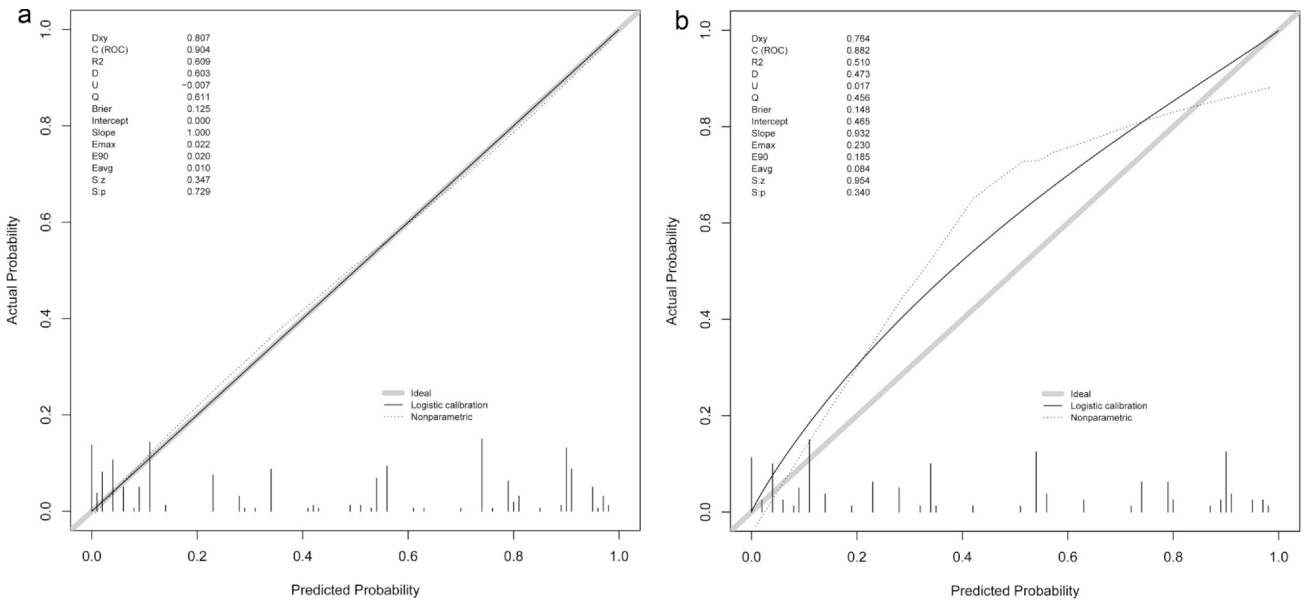

Figure 4. **(a–b)** Calibration curves of the nomogram for the training **(a)** and validation **(b)** cohorts. ROC, receiver operating characteristic.

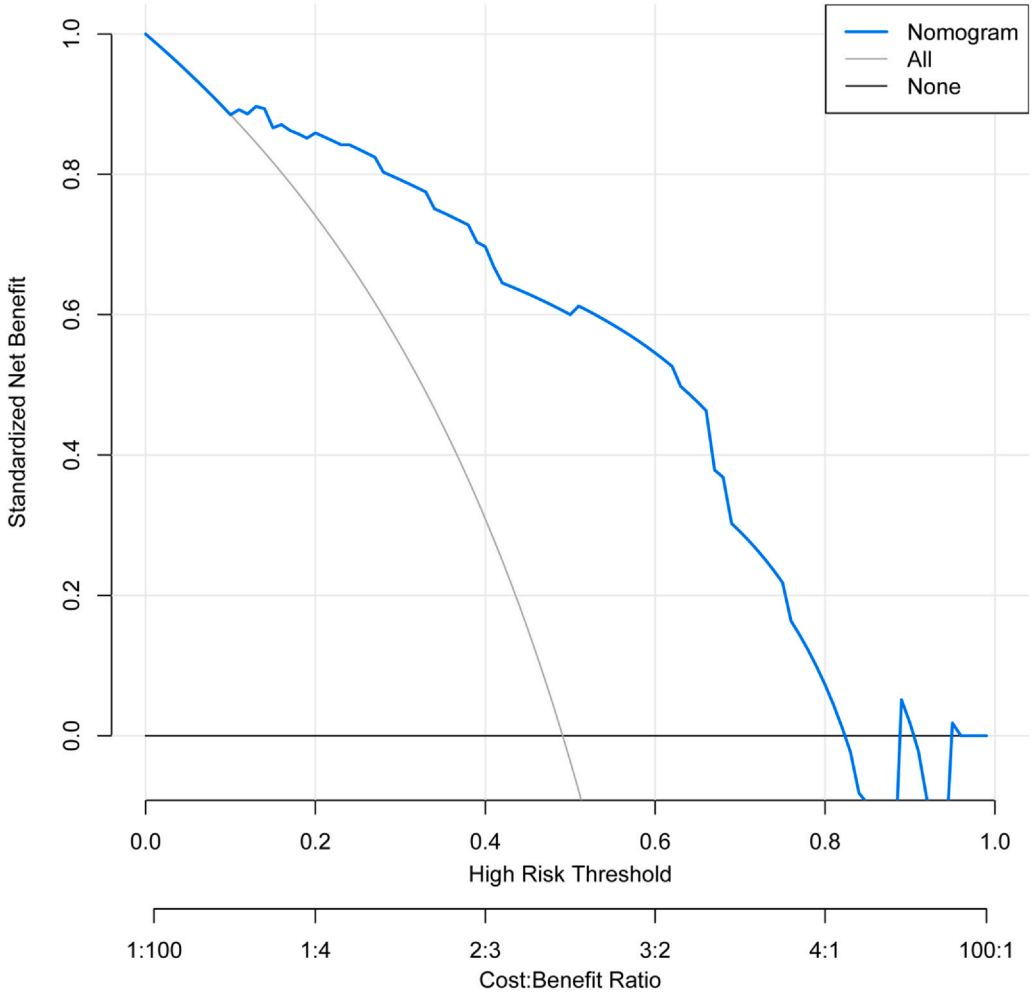

Figure 5. Decision curve analysis of the ultrasound nomogram. The x-axis represents the threshold probability, and the y-axis represents the net benefit.

TABLE 3. Agreement Among the Radiologists

Features	k
Maximum diameter	0.84
Range of peripheral calcification	0.81
Halo sign	0.76
Extrusion beyond calcification	0.81
Calcification continuity	0.78
Type of peripheral calcification	0.89
L/T ratio	0.76
Margin	0.81
Internal echogenicity	0.84
Composition	0.86
Internal calcification	0.87

0≤k≤0.4: poor; 0.41≤k≤0.75: fair to good; 0.76≤k < 1.0: excellent; k=1.0: perfect

and specificity of 60%–80% and 80%–90%, respectively (27). However, we found that an L/T ratio > 1 did not increase the risk of malignancy in nodules with peripheral calcification because peripheral calcified nodules may have limited infiltrative growth due to the presence of peripheral calcification.

Notably, among the 71 nodules with posterior acoustic shadowing, 24 (33.8%) were malignant. Therefore, the diagnosis of such nodules should be approached with caution, and the clinical application of these methods is somewhat limited. Therefore, for thyroid nodules with peripheral calcification, it is necessary to observe and analyze the signs associated with the calcification ring in addition to the ultrasound characteristics of the nodule. Our analysis showed that the continuity of peripheral calcification did not significantly differentiate benign lesions from malignant lesions, which is similar to the results of a recent study (10). The lack of significant results may be due to the difficulty in accurately assessing this feature. On the other hand, a study that included 19 benign and 45 malignant nodules (6) reported that interruption and thickening of peripheral calcification and reduced internal echogenicity of thyroid nodules were considered as risk factors for malignancy in nodules with peripheral calcification. Kim et al. analyzed 93 nodules with

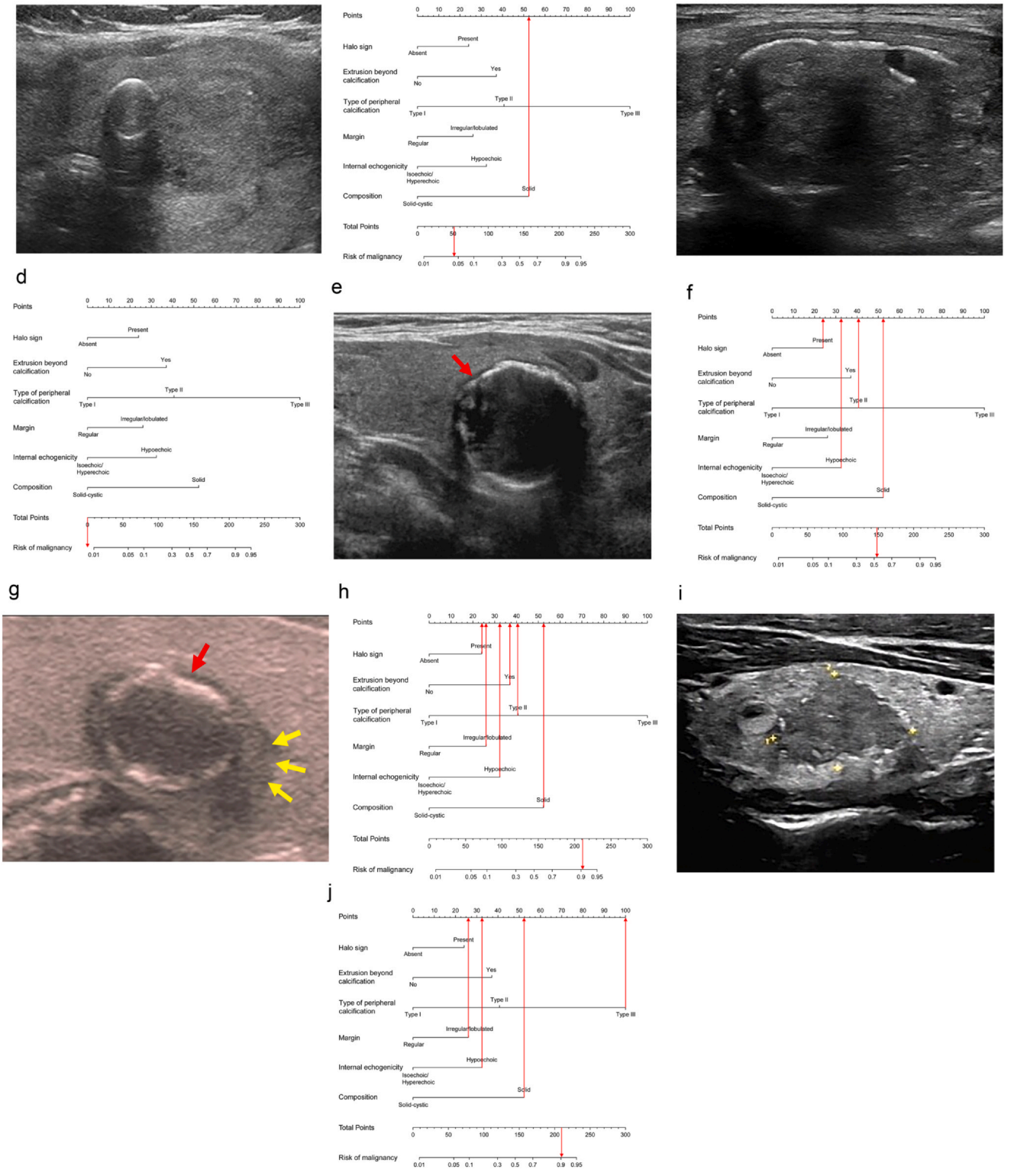

Figure 6. Examples of the clinical application of the US nomogram. **(a)** An image was obtained from a 63-year-old woman with a nodule of type I calcification in the left thyroid. **(b)** The nomogram resulted in a total score of 52 points for solid composition (52 points). The corresponding risk of malignancy was 0.04, and the pathological result of the nodule was benign by FNA. **(c)** An image was obtained from a 36-year-old woman with a nodule of type I calcification in the left thyroid. **(d)** The nomogram resulted in a total score of 0 points. The corresponding risk of malignancy was < 0.01, and the pathological result of the nodule was nodular goiter with adenomatous hyperplasia by surgery. **(e)** An image was obtained from a 45-year-old woman with a nodule of type II calcification in the right thyroid. The red arrow in the figure indicates the halo sign. **(f)** The nomogram resulted in a total score of 149 points for the halo sign (24 points), hypoechoic echogenicity (32 points), solid composition (52 points), and type II calcification (41 points). The corresponding risk of malignancy was 0.55 and the pathological result of the nodule was papillary carcinoma by surgery and FNA. **(g)** An image was obtained from a 68-year-old woman with a nodule of type II calcification in the right thyroid. The red arrow in the figure indicates the halo sign and the yellow arrow indicates the extrusion beyond calcification. **(h)** The nomogram resulted in a total score of 212 points for the halo sign (24 points), extrusion beyond calcification (37 points), hypoechoic echogenicity (32 points), solid composition (52 points), irregular margin (26 points), and type II calcification (41 points). The corresponding risk of malignancy was 0.91, and the pathological result of the nodule was papillary carcinoma by surgery and FNA. **(i)** An image was obtained from a 22-year-old man with a nodule of type III calcification in the left thyroid. **(j)** The nomogram resulted in a total score of 210 points for hypoechoic echogenicity (32 points), solid composition (52 points), irregular margin (26 points), and type III calcification (100 points). The corresponding risk of malignancy was 0.90, and the pathological result of the nodule was papillary carcinoma by FNA. FNA, fine-needle aspiration; US, ultrasound. (Color version of figure is available online.)

eggshell calcification and reported that the halo and disruption of eggshell-like calcification may be more useful than the hypoechoic, lobular margins, and high-width types (7). In our study, we found that a significant proportion (64.6%) of benign cases showed disruption of continuity, thus, we believe that the feature of continuity as a predictor of malignant nodules with peripheral calcification is not reliable. In contrast, we found extrusion beyond calcification was more likely to be an independent predictor than continuity. By examining the location of the peri-calcified tissue in relation to the nodule, we found that calcified rings in benign nodules were more often located at the margins of the nodule, whereas calcified rings located inside the nodule were more often seen in malignant nodules. Another point is that nodules exhibiting the feature of extrusion beyond the calcification ring are also frequently associated with irregular margins, which aligns with our findings mentioned previously. In addition, we found that the proportion of peripheral calcifications with halo signs around malignant thyroid nodules was significantly different from that around benign nodules, which is consistent with Kim's findings (7). Additionally, we found that the range of peripheral calcification was of no value in distinguishing benign nodules from malignant nodules, which is in agreement with the findings of Yoon (8).

In this study, the calcified rings were categorized into three types, with the most common type being type II (41.6%), followed by type I (36.8%) and type III (21.6%). 16 of the 140 type I lesions (11.4%) were malignant, 87 of the 158 type II lesions (55.1%), and 71 of the 82 type III lesions (86.6%) were malignant. Type I calcifications were more likely to occur in benign nodules, and type II and type III calcifications were more likely to occur in malignant nodules, with risk ratios of 4.4 and 36.7, respectively. We found that type II calcifications were more likely to be malignant than type I calcifications, suggesting that the increased thickness of the calcified ring indicates the likelihood of thyroid cancer, which may be due to the rapid deposition of the substances mentioned previously during the formation of malignant nodules. Given the biological characteristics of invasive growth, tumors may further penetrate and extrude the calcification ring. Additionally, the destruction of surrounding normal tissues by malignant nodules leads to the formation of hypoechoic halos, which is consistent with our findings mentioned previously. Therefore, Type II calcifications are more likely than Type I calcifications to exhibit features such as hypoechoic halos and extrusion beyond the calcification ring, thereby increasing the risk of malignancy. The relationship between calcification type and the malignancy of peripheral calcified nodules has also been studied, but the number of cases was relatively small. Kwak analyzed 21 cases of thyroid nodules with peripheral calcification and classified the nodules into peripheral nodular calcification, peripheral smooth-edge calcification, and peripheral irregular-edge calcification (13). 18 of the 21 nodules were confirmed to be papillary carcinomas, and there were no significant differences among the three types of calcifications. Yoon (8) retrospectively analyzed the ultrasonographic features of 65 pathologically confirmed peripheral calcifications of thyroid nodules, classified them into three types, and reported that there was no significant difference in the type of calcification between benign and malignant nodules.

It is worth mentioning that calcification type was the largest contributor to the scores in the nomogram and significantly enhanced model discrimination. Therefore, in our clinical practice, Type II and III calcified nodules warrant heightened vigilance. It is recommended to conduct comprehensive evaluations by integrating other US features (such as hypoechogenicity and solid components). Although Type I calcifications are predominantly benign, it remains essential to rule out other high-risk US features (e.g., irregular margins). In view of the clinical value of peripheral calcification typing, we believe that more studies are needed for in-depth exploration in the future: first, the biological mechanisms behind calcification typing need to be verified, such as whether the thickening of the calcification ring is correlated

with tumor angiogenesis; second, the current typing criteria need to be verified for their generalizability by multicenter studies. In addition, the predictive efficacy of the typing system can be further optimized by combining with molecular markers (e.g., BRAF mutation), so as to provide a more accurate biological basis for clinical decision-making.

This study has several limitations. First, this is a retrospective study, and potential selection bias is inevitable. Second, patients were enrolled from a single center, and a future multicenter study with a larger patient volume is needed. Finally, we performed only internal validation and not external validation to further evaluate the performance of the model.

CONCLUSION

In conclusion, the diagnosis of TNs with peripheral calcification is relatively challenging among all thyroid nodules and deserves sufficient clinical attention. We constructed a prediction model, including halo sign, extrusion beyond calcification, type of peripheral calcification, margin, internal echogenicity, and composition to differentiate malignant from benign thyroid nodules with peripheral calcifications. This model demonstrates strong discriminative ability, suggesting that it may be useful in identifying patients at high risk of malignancy, thereby guiding the need for more aggressive diagnostic procedures. Consequently, the nomogram could play a role in establishing future treatment recommendations for these patients.

DECLARATION OF COMPETING INTEREST

The authors declare that they have no known competing financial interests or personal relationships that could have appeared to influence the work reported in this paper.

ACKNOWLEDGMENT

This project was supported by International Science and Technology Cooperation Project of Shenzhen Science and Technology Innovation Committee (GJHZ20220913142801003) held by Professor Linghu Wu.

REFERENCES

1. Haugen B, Alexander E, Bible K. 2015 American Thyroid Association Management Guidelines for adult patients with thyroid nodules and differentiated thyroid cancer: the American Thyroid Association Guidelines Task Force on thyroid nodules and differentiated thyroid cancer. Thyroid 2016; 26(1):1–133.
2. Thyroid gland. In: Brunetin JN, editor. Medical Radiology: Radiological Imaging 01 Endocrine Diseases. *Berlin, Germany*: Springer-Verlag; 1999. p. 145–158.
3. Cheng SP, Lee JJ, Lin J, Liu CL. Eggshell calcification in follicular thyroid carcinoma. Eur Radiol 2005; 15(8):1773–1774. https://doi.org/10.1007/s00330-005-2676-2
4. Park CH, Rothermel FJ, Judge DM. Unusual calcification in mixed papillary and follicular carcinoma of the thyroid gland. Radiology 1976; 119(3):554. https://doi.org/10.1148/119.3.554
5. Vescini F, Di Gaetano P, Vigna E, et al. Anaplastic thyroid carcinoma in a 49 year-old woman with a long-standing goiter. A case report. Minerva Endocrinol 2000; 25(3-4):81–83.
6. Park M, Shin JH, Han BK, et al. Sonography of thyroid nodules with peripheral calcifications. J Clin Ultrasound 2009; 37(6):324–328. https://doi.org/10.1002/jcu.20584
7. Kim BM, Kim MJ, Kim EK, et al. Sonographic differentiation of thyroid nodules with eggshell calcifications. J Ultrasound Med 2008; 27(10):1425–1430. https://doi.org/10.7863/jum.2008.27.10.1425
8. Yoon DY, Lee JW, Chang SK, et al. Peripheral calcification in thyroid nodules: ultrasonographic features and prediction of malignancy. J Ultrasound Med 2007; 26(10):1349–1355. https://doi.org/10.7863/jum.2007.26.10.1349
9. MS K, JH B, YS K, et al. Patterns and significance of peripheral calcifications of thyroid tumors seen on ultrasound. J Korean Radiol Soc 2005; 53:401–405.
10. Malhi HS, Velez E, Kazmierski B, et al. Peripheral thyroid nodule calcifications on sonography: evaluation of malignant potential. AJR Am J Roentgenol 2019; 213(3):672–675. https://doi.org/10.2214/ajr.18.20799
11. JL F, B L, MC P. Statistical methods for rates and proportions. 2nd edition.., *New York*: John Wiley & Sons Ltd,; 1981.
12. Taki S, Terahata S, Yamashita R, et al. Thyroid calcifications: sonographic patterns and incidence of cancer. Clin Imaging 2004; 28(5):368–371. https://doi.org/10.1016/s0899-7071(03)00190-6
13. Kwak JY, Han KH, Yoon JH, et al. Thyroid imaging reporting and data system for US features of nodules: a step in establishing better stratification of cancer risk. Radiology 2011; 260(3):892–899. https://doi.org/10.1148/radiol.11110206
14. Remonti LR, Kramer CK, Leitão CB, et al. Thyroid ultrasound features and risk of carcinoma: a systematic review and meta-analysis of observational studies. Thyroid 2015; 25(5):538–550. https://doi.org/10.1089/thy.2014.0353
15. Haugen BR, Alexander EK, Bible KC, et al. 2015 American Thyroid Association Management Guidelines for adult patients with thyroid nodules and differentiated thyroid cancer: the American Thyroid Association Guidelines Task Force on thyroid nodules and differentiated thyroid cancer. Thyroid 2016; 26(1):1–133. https://doi.org/10.1089/thy.2015.0020
16. Tessler FN, Middleton WD, Grant EG, et al. ACR thyroid imaging, reporting and data system (TI-RADS): white paper of the ACR TI-RADS committee. J Am Coll Radiol 2017; 14(5):587–595. https://doi.org/10.1016/j.jacr.2017.01.046
17. Guo BL, Ouyang FS, Ouyang LZ, et al. Development and validation of an ultrasound-based nomogram to improve the diagnostic accuracy for malignant thyroid nodules. Eur Radiol 2019; 29(3):1518–1526. https://doi.org/10.1007/s00330-018-5715-5
18. Ren JY, Lv WZ, Wang L, et al. Dual-modal radiomics nomogram based on contrast-enhanced ultrasound to improve differential diagnostic accuracy and reduce unnecessary biopsy rate in ACR TI-RADS 4-5 thyroid nodules. Cancer Imaging 2024; 24(1):17. https://doi.org/10.1186/s40644-024-00661-3
19. Yousefi E, Sura GH, Somma J. The gray zone of thyroid nodules: Using a nomogram to provide malignancy risk assessment and guide patient management. Cancer Med 2021; 10(8):2723–2731. https://doi.org/10.1002/cam4.3866
20. Pizzato M, Li M, Vignat J, et al. The epidemiological landscape of thyroid cancer worldwide: GLOBOCAN estimates for incidence and mortality rates in 2020. Lancet Diabetes Endocrinol 2022; 10(4):264–272. https://doi.org/10.1016/s2213-8587(22)00035-3
21. Siegel RL, Miller KD, Wagle NS, et al. Cancer statistics, 2023. CA Cancer J Clin 2023; 73(1):17–48. https://doi.org/10.3322/caac.21763
22. Li M, Dal Maso L, Vaccarella S. Global trends in thyroid cancer incidence and the impact of overdiagnosis. Lancet Diabetes Endocrinol 2020; 8(6):468–470. https://doi.org/10.1016/s2213-8587(20)30115-7
23. Sung H, Ferlay J, Siegel RL, et al. Global Cancer Statistics 2020: GLOBOCAN estimates of incidence and mortality worldwide for 36

cancers in 185 countries. CA Cancer J Clin 2021; 71(3):209–249. https://doi.org/10.3322/caac.21660
24. Lee YH, Baek JH, Jung SL, et al. Ultrasound-guided fine needle aspiration of thyroid nodules: a consensus statement by the Korean society of thyroid radiology. Korean J Radiol 2015; 16(2):391–401. https://doi.org/10.3348/kjr.2015.16.2.391
25. Sharma A, Gabriel H, Nemcek AA, et al. Subcentimeter thyroid nodules: utility of sonographic characterization and ultrasound-guided needle biopsy. AJR Am J Roentgenol 2011; 197(6):W1123–W1128. https://doi.org/10.2214/ajr.10.5684
26. Kim MJ, Kim EK, Park SI, et al. US-guided fine-needle aspiration of thyroid nodules: indications, techniques, results. Radiographics 2008; 28(7):1869–1886. https://doi.org/10.1148/rg.287085033
27. Gharib H, Papini E, Garber JR, et al. American Association of Clinical Endocrinologists, American College of Endocrinology, and Associazione Medici Endocrinologi Medical Guidelines for Clinical Practice for the Diagnosis and Management of Thyroid Nodules–2016 update. Endocr Pract 2016; 22(5):622–639. https://doi.org/10.4158/ep161208.GI